Low dielectric loss ceramics in the $Mg_4Nb_2O_9$-$ZnAl_2O_4$-TiO_2 ternary system

Yu-Chuan Wu[1], Hsiao-Ting Tseng[2], Chi-Shiung Hsi[2], Jari Juuti [3], Hsing-I Hsiang[4, *]

[1] Department of Materials and Mineral Resources Engineering, National Taipei University of Technology, Taipei, Taiwan

[2] Department of Materials Science and Engineering, National United University, Miaoli, Taiwan

[3] Microelectronics and Materials Physics Laboratory, Department of Electrical Engineering, University of Oulu, Oulu90014, Finland

[4] Department of Resources Engineering, National Cheng Kung University, Tainan, Taiwan

*: corresponding author, email: hsingi@mail.ncku.edu.tw

Abstract

This study used a traditional solid-state reaction method to prepare a series of composite ceramics in the $0.7Mg_4Nb_2O_9$-$(0.3-x)ZnAl_2O_4$-$xTiO_2$ ternary system. Crystalline phases and microstructure of $Mg_4Nb_2O_9$-$ZnAl_2O_4$-TiO_2 dielectric ceramic composites were investigated and correlated with the relevant dielectric properties. It was observed that the addition of Ti^{4+} substituted Nb^{5+} in the $Mg_4Nb_2O_9$ structure, which promoted the decomposition of $Mg_4Nb_2O_9$ to form the second phase, $Mg_5Nb_4O_{15}$, during sintering. The synergistic effect of $ZnAl_2O_4$-TiO_2 co-doping promoted the $Mg_4Nb_2O_9$

ceramic densification. The sample ($0.7Mg_4Nb_2O_9$-$(0.3-x)ZnAl_2O_4$-$xTiO_2$) with x = 0.15-0.2 exhibited dielectric constants of 13-14, larger than those of $ZnAl_2O_4$, $Mg_4Nb_2O_9$ and $Mg_5Nb_4O_{15}$, due to the NbO_6 octahedra distortion resulting from the substitution of Al^{3+}/Ti^{4+} for Nb^{5+} in $Mg_4Nb_2O_9$ and $Mg_5Nb_4O_{15}$. The long-range order of the NbO_6 octahedra was enhanced by co-doping $ZnAl_2O_4$ and TiO_2, thereby enhancing the Qxf value. A dielectric constant of 13.1, Qxf value of 366,000 GHz and a τ_f of −60.8ppm/°C were obtained from 1300°C sintered $0.7Mg_4Nb_2O_9$-$0.15ZnAl_2O_4$-$0.15TiO_2$. These results show that $0.7Mg_4Nb_2O_9$-0.15 $ZnAl_2O_4$-$0.15TiO_2$ ceramic is a good candidate for microwave electronic device applications.

Keywords: dielectric loss, $Mg_4Nb_2O_9$, $ZnAl_2O_4$, TiO_2, microwave ceramics

1. Introduction

Low-permittivity dielectric ceramics are used for millimeter-wave communication and as microwave ceramic substrates. As the permittivity decreases, the signal transmission speed increases. Dielectric ceramics with properties of temperature-stability, low-permittivity and a high Qxf are required in millimeter-wave applications. High Qxf dielectric ceramics minimize circuit insertion losses and can be used for highly selective filters. Searching for new microwave dielectric ceramics with high-temperature stability, low permittivity, high Qxf and low cost has always attracted much attention [1-3]. The microwave dielectric properties of ceramics are determined by several

parameters, including the phase composition, the processing conditions and their ultimate densification/porosity [4]. One effective method for obtaining a lower temperature-sintered microwave dielectric ceramic with high Qxf and near-zero τ_f values is by adding low-temperature-fired ceramics to the dielectric [5-6].

Ogawa et al. [7] first reported the microwave dielectric properties (ε_r = 12.4, Qxf ~ 19,400 GHz, τ_f = −70 ppm/°C) of $Mg_4Nb_2O_9$ ceramics sintered at 1400°C for 10 h. $Mg_4Nb_2O_9$ ceramic exhibits an ordered corundum structure in which the NbO_6 octahedral layer along the c axis is separated by the MgO_6 octahedral layer and the cation vacancy layer. In contrast, the NbO_6 octahedral layer along the b axis is sandwiched by two MgO_6 octahedral layers [8]. $Mg_4Nb_2O_9$ ceramics have gained much attention due to their high Qxf and low ε_r value [9-11]. However, the drawbacks of $Mg_4Nb_2O_9$ ceramics, such as a higher sintering temperature and a significant negative τ_f, adversely affect their application. The addition of TiO_2 with positive τ_f to $Mg_4Nb_2O_9$ ceramics has been used to improve the τ_f [12].

$ZnAl_2O_4$ ceramic exhibiting a spinel structure has been considered a potential microwave ceramic substrate material [13-15]. Surendran et al. first reported the microwave dielectric properties (ε_r = 8.5, Qxf ~ 56,300 GHz, τ_f = −79 ppm/°C) of $ZnAl_2O_4$ ceramic [13]. Zheng et al. [14] reported that good dielectric properties (ε_r = 8.56, Qxf = 106,000 GHz and τ_f = −63 ppm/°C) can be obtained for 1650°C sintered

$ZnAl_2O_4$ ceramic. The Q×f of $ZnAl_2O_4$ ceramic sintered at 1600°C was enhanced by forming a $(Zn_{1-x}Mg_x)Al_2O_4$ solid solution which reached above 140,000 GHz [15]. The addition of 2 wt% TiO_2 promoted the densification and dielectric properties of $Zn_{0.9}Mg_{0.1}Al_2O_4$ sintered at 1500°C (ε_r = 8.57, Qxf ~ 180,800 GHz, τ_f = −41.5 ppm/°C) [16].

Due to crystal structure differences, $Mg_4Nb_2O_9$, $ZnAl_2O_4$ and TiO_2 cannot form a solid solution, instead forming ceramic matrix composites with adjustable dielectric properties. The proper addition of $ZnAl_2O_4$ and TiO_2 may promote the densification, improve the quality factor and compensate the temperature coefficient (τ_f) of $Mg_4Nb_2O_9$ ceramics. To our knowledge, there are very few reported investigations into the behaviour of the $Mg_4Nb_2O_9$- $ZnAl_2O_4$-TiO_2 composites which might exhibit promising features for microwave dielectric ceramics. In a previous study, the $xMg_4Nb_2O_9$-(1-x)/2$ZnAl_2O_4$-(1-x)/2TiO_2 (x = 0.4-0.8) ternary system with quality factors between 10,500 and 120,000 was investigated [17]. This study designed and prepared a series of composite ceramics in the $0.7Mg_4Nb_2O_9$-(0.3-x)$ZnAl_2O_4$-xTiO_2 ternary system via a traditional solid-state reaction method. Crystalline phases and microstructure of $Mg_4Nb_2O_9$-$ZnAl_2O_4$-TiO_2 dielectric ceramic composites were investigated and correlated with the relevant dielectric properties.

2. Experimental procedure

According to the stoichiometric ratio of $Mg_4Nb_2O_9$ and $ZnAl_2O_4$, barium niobate and zinc aluminate powders were prepared via the mixed oxides process with reagent-grade MgO, Nb_2O_5, ZnO and Al_2O_3. The calcination conditions of $Mg_4Nb_2O_9$ powder were held at a temperature of 1300°C for 3h. The $ZnAl_2O_4$ powder was calcined at 1200°C for 2h. The $0.7Mg_4Nb_2O_9$-$yZnAl_2O_4$-$xTiO_2$ ternary systems; (MZ015: x = 0, y=0.15), (MZT015: x = 0.15, y=0.15), (MZT175: x = 0.175, y=0.125), (MZT020: x = 0.2, y=0.1) and (MT015: x = 0.15, y=0) were prepared from mixtures of reagent-grade TiO_2, $Mg_4Nb_2O_9$ and $ZnAl_2O_4$ powders, and the mixed powders were then milled for 3 h using Y-TZP balls. The milled powders were dried in an oven and PVA was then added for granulation. The powders were uniaxially pressed at 255 MPa into disks of 10 mm diameter and 5 mm thickness. These pressed disks were debinded at 450°C for 1 h and sintered at 1250°C - 1500°C for 3 h.

The crystalline phases of sintered pellets were determined by X-ray diffractometry (Brucker, D2 Phaser, Cu-Kα radiation, Karisruhe, Germany). The relative fractions of the constituent phases were quantitatively analyzed from the XRD data using Bruker Topas v4.2 software. The relative densities were calculated from the ratios of apparent density and true density of the sintered disks. Archimedes' method was used to measure the apparent densities of the sintered samples. The sintered disks

were ground into powder and the true densities of the ground powders were measured using helium pycnometry (Quantachrome, ULTRAPYC 1200e, Boynton Beach, FL, USA). Scanning electron microscopy (JEOL JSM-5600F, Tokyo, Japan), transmission electron microscopy (JEOL, JSM-2100F, Tokyo, Japan) and energy dispersive spectroscopy (EDS, Oxford Instruments, 6587, High Wycombe, UK) were used to observe the sintered pellets' microstructure, crystalline phase and chemical composition. For SEM analysis, the surface of the ceramics was ground using SiC 1200 grit paper and polished using diamond paste. The polished samples were then thermally etched at 1200°C for 5 min in air. Thin foils for TEM observation were prepared via the conventional technique: the sintered disks were sliced to a thickness of ~200 μm and then mechanically polished to a thickness of ~30 μm followed by ion-beam thinning to electron transparency. Raman spectra were measured by a Raman spectrometer (Dong Woo 500i, Gyeonggi-do, South Korea) with conditions of a detecting time of 50 s and resolution of 1 cm^{-1}. Samples were excited by an Ar ion laser beam with a wavelength of 532 nm and power output of 35 mW.

The relative permittivity (ε_r) and quality factor (Q) at microwave frequency were measured with the Hakki-Coleman dielectric resonator method using a HP8757D (Agilent Technologies, Palo Alto, CA) network analyzer and a HP8350B (Agilent Technologies) sweep oscillator. The Q value was measured using the TE011 resonant

peak and τ_f was obtained by measuring the resonant frequency in the temperature range of 25–85°C. The τ_f value (ppm/°C) was calculated by noting the change in resonant frequency.

3. Results and discussion

Figure 1 shows the XRD patterns of the MZT015 sintered at various temperatures. All the samples had a well-defined main phase; Mg_4Nb_2O, a minor phase of $ZnAl_2O_4$ and an evident second phase of $Mg_5Nb_4O_{15}$ were observed. The diffraction peak of the TiO_2 phase was not observed in the XRD profiles. Su et al. [12], who reported that the $Mg_5Nb_4O_{15}$ phase formed after sintering of $Mg_4Nb_2O_9$ with TiO_2 as an additive, also observed consistent results. The diffraction angles of $Mg_4Nb_2O_9$ and $Mg_5Nb_4O_{15}$ phases shifted to higher values as the sintering temperature increased. This suggested that the unit cell volumes of $Mg_4Nb_2O_9$ and $Mg_5Nb_4O_{15}$ decreased with increasing sintering temperature [18-19]. Table S1 (supplementary materials) shows the lattice parameters of the MZT015 sintered at various temperatures. The lattice parameters of $Mg_4Nb_2O_9$ and $Mg_5Nb_4O_{15}$ decreased with increasing sintering temperature due to the increase in the ion substitution of Ti^{4+} (ionic radius = 0.60 nm) for Nb^{5+} (ionic radius = 0.61 nm) [20]. Table S2 (supplementary materials) shows the phase content of the samples sintered at 1300°C . As the TiO_2 content increased from 15 mol% to 20 mol%, the content of the $Mg_5Nb_4O_{15}$ phase increased from 32.2 wt% to 41.3 wt% in the

$0.7Mg_4Nb_2O_9$-$(0.3-x)ZnAl_2O_4$-$xTiO_2$ ternary system, while the content of the $ZnAl_2O_4$ phase remained almost unchanged (at about 5 wt%). The amounts of the $Mg_5Nb_4O_{15}$ phase in MZ015 and MT015 were 12.7 wt% and 45.5 wt%, respectively. The phase diagram of Nb_2O_5-MgO predicts that the $Mg_4Nb_2O_9$ and $Mg_5Nb_4O_{15}$ coexist at equilibrium because the molar ratio of Nb_2O_5 to MgO is slightly larger than 20/80 [21]. These results suggest that the addition of Ti^{4+} dissolved in $Mg_4Nb_2O_9$ mainly replaced Nb^{5+}, which thus promoted the decomposition of $Mg_4Nb_2O_9$ and formed the second phase of $Mg_5Nb_4O_{15}$ [12].

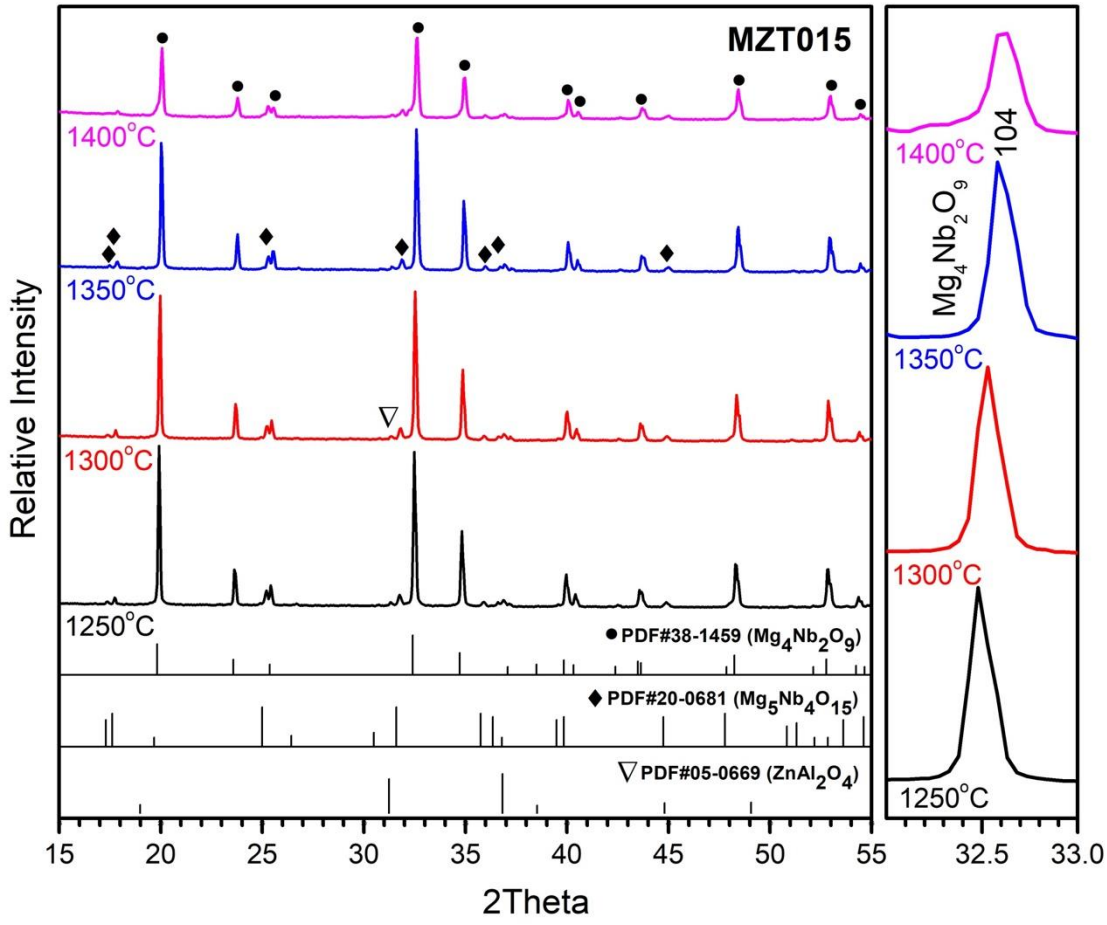

Fig. 1 XRD patterns of the MZT015 dielectric ceramics sintered at various temperatures.

Figure 2 shows the relative densities of the samples sintered at various temperatures. For the MZ015 and MT015 sintered disks, the relative densities were not greater than 90% until the sintering temperature reached 1400°C. The samples in the $0.7Mg_4Nb_2O_9$-$(0.3-x)ZnAl_2O_4$-$xTiO_2$ ternary system initially had relative densities higher than 95%. These increased slightly with increasing sintering temperature and reached a maximum value in the sintering temperature range from 1300°C to 1350°C. Based on the system of Nb_2O_5-MgO, the liquidus temperature decreases when increasing the molar ratio of Nb_2O_5 to MgO in the coexistence region of $Mg_4Nb_2O_9$ and $Mg_5Nb_4O_{15}$ [21]. The addition of Ti^{4+} substituting Nb^{5+} in the $Mg_4Nb_2O_9$ structure made the sintered samples become Nb-excess and decreased the liquidus temperature. The addition of Ti^{4+} reduced the liquidus temperature, which reduced the activation energy of sintering and high sinterability at a low temperature [22]. Huang et al. [23] developed low-loss microwave dielectrics using $(Mg_{1-x}Zn_x)_4Nb_2O_9$ solid solution; they concluded that the addition of Zn^{2+} decreased the densification temperature of $(Mg_{1-x}Zn_x)_4Nb_2O9$ dielectric from 1400°C to 1340°C. The synergistic effect of the $ZnAl_2O_4$-TiO_2 co-doping enhancing the densification of $Mg_4Nb_2O_9$ ceramics was observed in this study.

At a sintering temperature of 1300°C, the MZT015 sample exhibited the highest relative densities compared with other compositions.

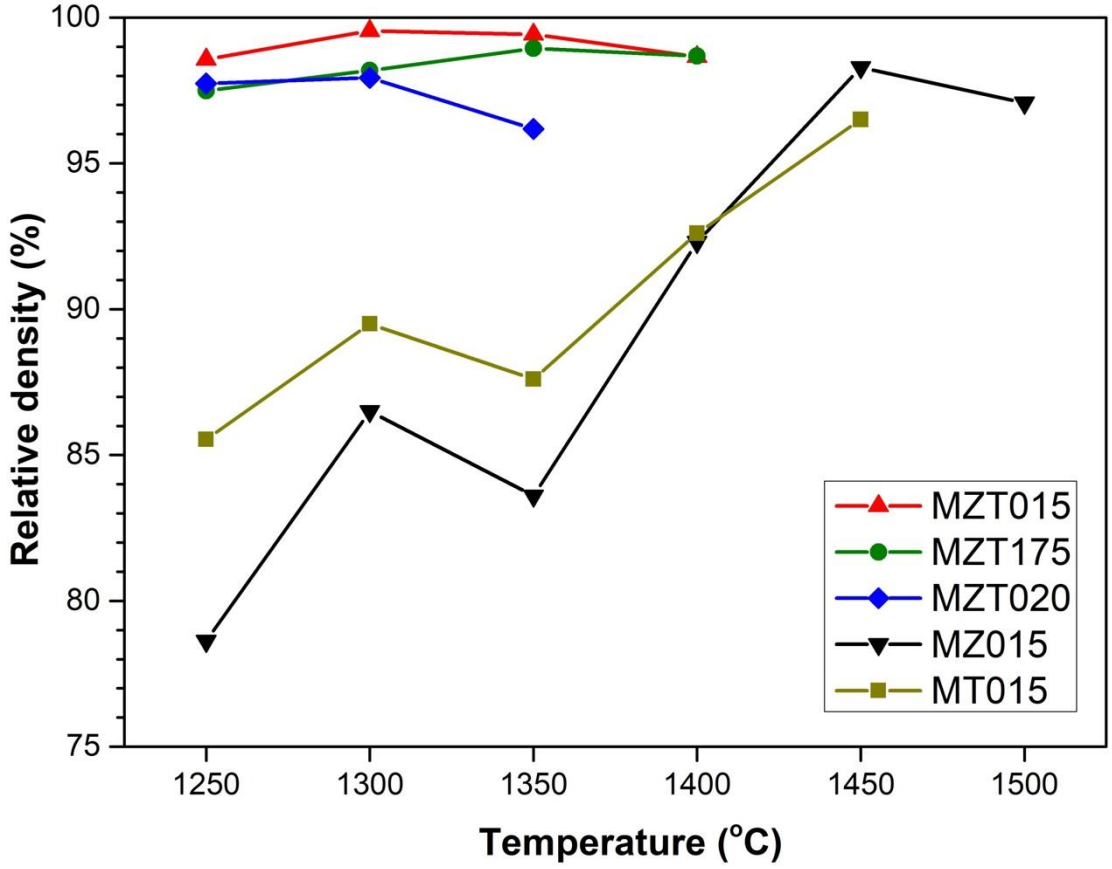

Figure 2 Relative densities of the $0.7Mg_4Nb_2O_9$-$yZnAl_2O_4$-$xTiO_2$ ternary dielectrics sintered at various temperatures.

The SEM micrographics of the MZT015 sintered at various temperatures and MZT175 sintered at 1400°C are shown in Figure 3. All samples exhibited a dense microstructure, which is consistent with the relative sintered density results. The incidence of large and elongated matrix grains was increased by increasing the sintering temperature. The MTZ015 sample sintered at 1250°C for 3 h had a grain size around 5 μm, as shown in Fig 3(a). When the sample was sintered at 1350°C for 3 h, the grains in the sintered

pellet became elongated with dimensions larger than 10 μm, as indicated in Fig 3(c). The MTZ175 sintered at 1400°C for 3 h had a matrix grain size larger than 15 μm, as shown in Fig 3(d). Precipitates with small grain size located inside the grains as intragranular precipitates, and also at the grain boundaries or triple junctions, were observed. The EDS analysis results obtained from the regions marked A, B and C in Fig. 3(d) are tabulated in Table S3 (supplementary materials). The (Mg+Zn) to (Nb+Al+Ti) molar ratio of large matrix grains was 2.1, corresponding to the composition of $Mg_4Nb_2O_9$. The intragranular precipitate, point B in Fig 3(d), had an (Mg+Zn) to (Nb+Al+Ti) molar ratio of 1.18 and was compatible with the composition of $Mg_5Nb_4O_{15}$. The grain located at the triple junction, as indicated by the arrow in Fig 3(d), had an (Mg+Zn) to (Nb+Al+Ti) molar ratio of 0.56. It had a very low Nb^{5+} content, which was considered as a $(Mg/Zn)Al_2O_4$ solid solution based on the XRD analysis results (Figure 1). The $Mg_5Nb_4O_{15}$ and $ZnAl_2O_4$ phases existed in the 1300°C sintered MZT015 sample and can also be identified by the HRTEM images, diffraction patterns and the corresponding fast Fourier transform (FFT) patterns (Fig. S1, supplementary materials).

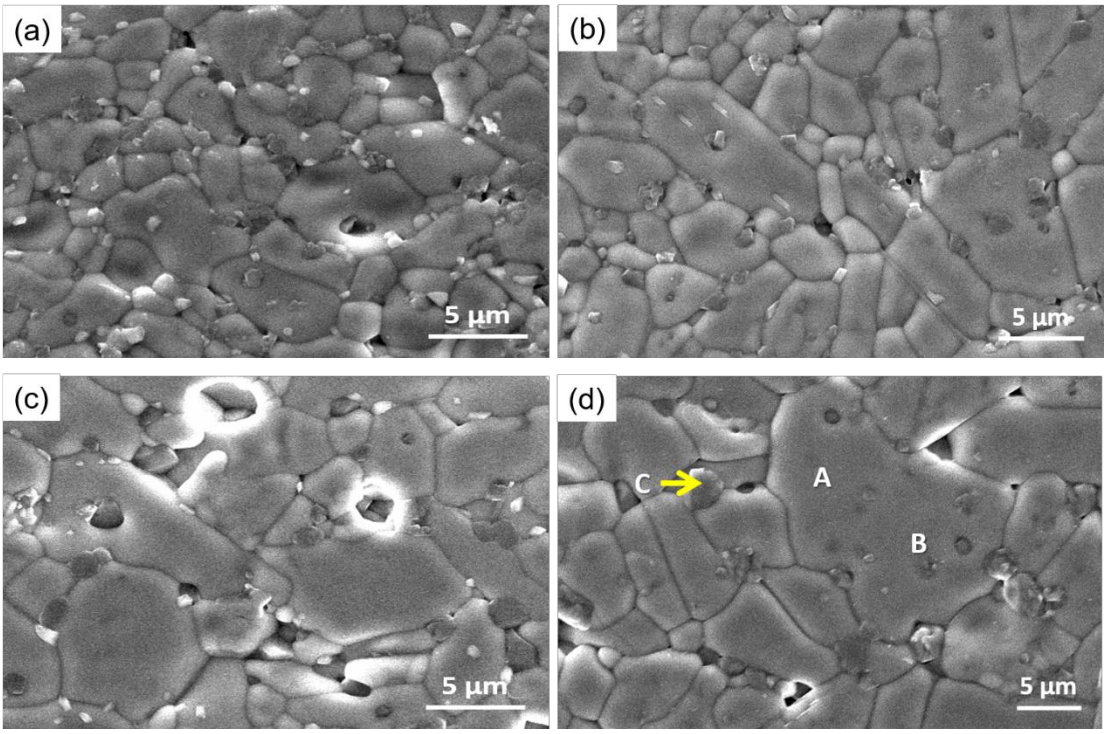

Fig. 3 SEM microstructures of the MZT015 sintered at various temperatures (a) 1250°C, (b)1300°C, (c) 1350°C, and (d) MZT175 sintered at 1400°C.

The previous paragraph suggests that a large proportion of Al^{3+} in the $ZnAl_2O_4$ and Ti^{4+} in the TiO_2 diffused into the $Mg_4Nb_2O_9$ lattice and a large proportion of Mg^{2+} migrated into the $ZnAl_2O_4$ from the $Mg_4Nb_2O_9$. As the chemical composition of $Mg_4Nb_2O_9$ changes from stoichiometric to Nb-rich phase, the single $Mg_4Nb_2O_9$ phase becomes the mixture phases of $Mg_4Nb_2O_9$ and $Mg_5Nb_4O_{15}$[21]. Bezjak et al. [24] investigated the synthesis and polymorphic phase transition of $Ba_4Nb_2O_9$ and observed that well-crystallized hexagonal $Ba_4Nb_2O_9$ grains tended to decompose into BaO-rich amorphous phase and nanocrystalline $Ba_5Nb_4O_{15}$ during sintering. They inferred that the substitution of Al^{3+} and Ti^{4+} for Nb^{5+} in $Mg_4Nb_2O_9$ may promote the decomposition of

$Mg_4Nb_2O_9$ into $Mg_5Nb_4O_{15}$ and that the MgO-rich amorphous phase easily reacts with $ZnAl_2O_4$ and forms $(Mg/Zn)Al_2O_4$ solid solution.

The Raman spectra of $Mg_4Nb_2O_9$ and MZT015 sintered samples are displayed in Fig. 4. Strong Raman active modes were observed at 330 cm^{-1}, 380 $cm^{-1,}$ and 810 cm^{-1}, which were assigned to the symmetric bending modes (F_{2g} mode) and stretching modes (A_{1g} mode) of NbO_6 octahedra with Oh symmetry, respectively [25]. The significant distortion of NbO_6 octahedra resulted in the Raman peak broadening or splitting. At about 810 cm^{-1}, A_{1g} mode, the strongest band was ascribed to the shortest Nb-O bond length. Sample MZT015 displayed the A_{1g} mode split into three Raman-active modes. This was attributed to the presence of different Nb-O bond distances resulting from the coexistence of $Mg_4Nb_2O_9$ and $Mg_5Nb_4O_{15}$. In addition, a higher wave number of the A_{1g} mode in MZT015 (818 cm^{-1}) was observed compared with $Mg_4Nb_2O_9$ (812 cm^{-1}). This was due to the decrease in the oxygen octahedron size [26] resulting from the Ti^{4+} substituting Nb^{5+}. The F_{2g} mode is associated with the internal vibrations of an oxygen octahedron. Figure 4 shows the F_{2g} mode split into a doublet at 330 and 380 cm^{-1} due to the empty octahedra resulting from a slight local departure from the $P\bar{3}c1$ space group [27]. This was expected to be split due to the distortion of NbO_6 octahedra for MZT015. Phonons of MZT015 and $Mg_4Nb_2O_9$ exhibited nearly the same peak position of the F_{2g} mode; this was because the F_{2g} mode was not affected by the slight lattice

distortions reported by Siny et al. [28]. The F_{2g} mode is only sensitive to long-range order on the NbO_6 octahedra, while the A_{1g} mode is caused by either long-range or short-range order [29]. The narrower band width and higher intensity of the F_{2g} mode are characteristic of the enhanced level of ordering. MZT015 exhibited higher intensities and a narrower peak width of the F_{2g} mode than $Mg_4Nb_2O_9$, suggesting that long-range order was enhanced for sample MZT015. This may be due to the aliovalent Al^{3+}/Ti^{4+} cations and Nb^{5+} that tend to occupy specific NbO_6 octahedron sites to decrease the lattice strain, resulting in an ordered crystal structure [28].

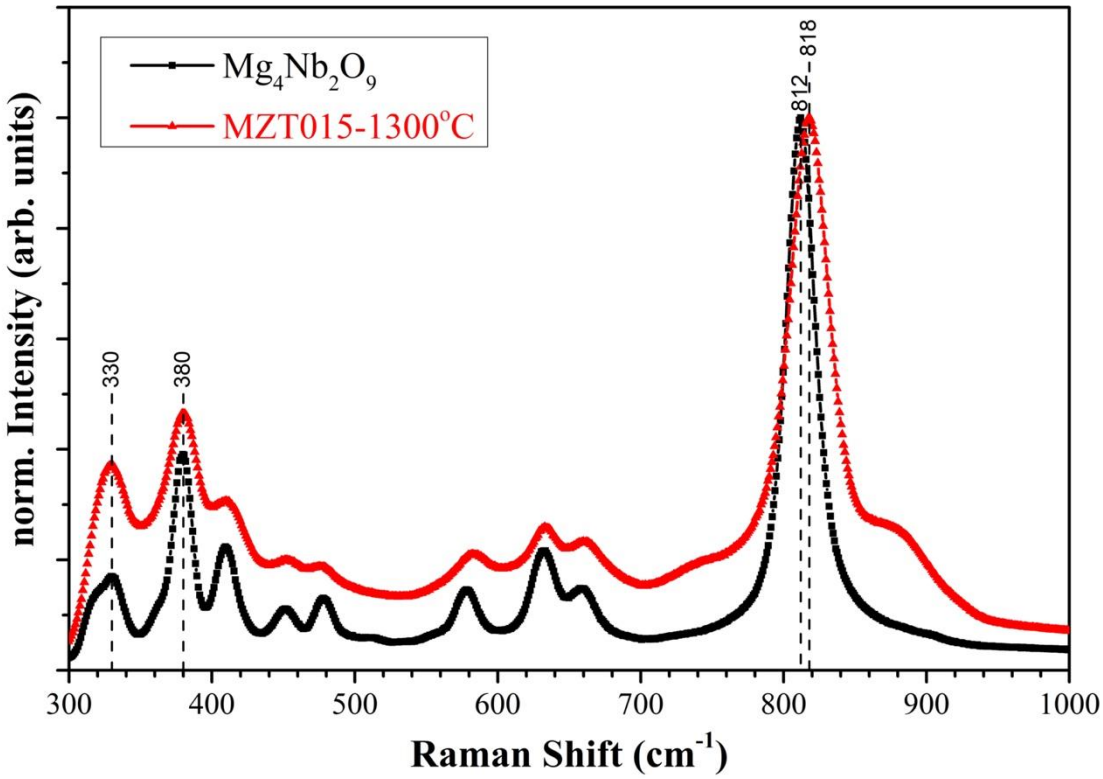

Fig.4 Raman spectra of $Mg_4Nb_2O_9$ and MZT015 sintered at 1300°C.

Table I shows the variation of the dielectric properties of the samples with different sintering temperatures. The dielectric properties of $Mg_4Nb_2O_9$, $Mg_5Nb_4O_{15}$, $ZnAl_2O_4$

and TiO_2 reported in the literature are tabulated in Table II. It is well known that the relative density and phase constituent determine the dielectric constant. The dielectric constant of the sample MZ015, without the addition of TiO_2 ($\varepsilon_r = 105$), was 12.8, which was the lowest among these samples owing to the highest number of pores ($\varepsilon_r = 1$). As listed in Table II, the dielectric constants of $Mg_4Nb_2O_9$, $Mg_5Nb_4O_{15}$, $ZnAl_2O_4$ and $MgAl_2O_4$ phases are all lower than 13. The MZT sample (0.7 $Mg_4Nb_2O_9$-(0.3-x) $ZnAl_2O_4$-xTiO_2) with x = 0.15-0.2 and the MT015 samples exhibited dielectric constants between 13 and 14. This is due to the larger NbO_6 octahedra distortion [27] resulting from the substitution of Al^{3+}/Ti^{4+} for Nb^{5+} in $Mg_4Nb_2O_9$ and $Mg_5Nb_4O_{15}$, thereby resulting in a higher dielectric constant. The Qxf value is dependent on the relative density, constituent phase and the ordering of cations in NbO_6 octahedra [4]. The Qxf value of the samples increased with increasing sintering temperature and reached a maximum value, then declined, which showed a similar trend to that of the relative density behaviour. The maximum Qxf value for the MZT015, MZT175 and MZT020 samples were 366,000, 296,000 and 176,000, respectively. The maximum Qxf value decreased with the increase of the TiO_2 addition, which was due to the amount of the second phase, $Mg_5Nb_4O_{15}$, which increased with increasing TiO_2 addition.

Table I Dielectric properties of the samples sintered at different temperatures.

	MZT015	MZT175	MZT020	MT015	MZ015

Sintering Temperature (°C)	ε_r	Qxf*	τ_f^+	ε_r	Qxf	ε_r	Qxf	ε_r	Qxf	ε_r	Qxf
1250	13.6	208k	-	13.6	230k	13.8	147k	-	-	-	-
1300	13.1	366k	-60.8	13.7	296k	13.6	66k	-	-	-	-
1350	13.1	325k	-62.3	13.5	274k	13.2	32k	-	-	-	-
1400	13.2	341k	-64.3	13.2	122k	-	-	13.0	16.2k	12.8	13.7k

*unit of Qxf: GHz, +unit of τ_f: ppm/°C

Table II Dielectric properties of $Mg_4Nb_2O_9$, $ZnAl_2O_4$, TiO_2, $Mg_5Nb_4O_{15}$, and $MgAl_2O_4$ reported in the literature

Materials	**ε_r**	**Q×f(GHz)**	**τ_f (ppm/°C)**	**ref**
$Mg_4Nb_2O_9$	12.4	192268	-70.5	Yoshida [9]
$ZnAl_2O_4$	8.5	56300	−79	Huang [15]
TiO_2	105	17600	411	Surendran [13]
$Mg_5Nb_4O_{15}$	11.3	43300	-58	Wu [30]
$MgAl_2O_4$	8.75	68900	-75	Surendran [31]

Since the $Mg_4Nb_2O_9$ phase exhibited a higher Qxf value than the $Mg_5Nb_4O_{15}$, the presence of the second phase, $Mg_5Nb_4O_{15}$, degraded the Qxf value of the samples. The MZT015 and MZT175 sintered disks exhibited higher Qxf values than those of the end

members. The ordering of cations in NbO_6 octahedra has been shown to dominate the Qxf value [32]. The substitution of aliovalent Al^{3+}/Ti^{4+} for Nb^{5+} enhanced the long-range order of NbO_6 octahedra for MZT015 and MZT175, which had a significantly beneficial effect on Qxf values. Huang et al. [23] reported that the substitution of Zn^{2+} for Mg^{2+} in $Mg_4Nb_2O_9$ can also substantially increase the Q×f value. Moreover, the Q×f value of $ZnAl_2O_4$ ceramic could be significantly improved by forming a $(Zn_{1-x}Mg_x)Al_2O_4$ solid solution [15]. Therefore, a low dielectric loss $Mg_4Nb_2O_9$ ceramic can be obtained by co-doping the proper amount of $ZnAl_2O_4$ and TiO_2. The τ_f is mainly determined by the relative sintered density and the constituent phase. For MZT015, the τ_f was about -60 ppm/°C and almost independent of the sintering temperature due to there being no significant constituent phase change. It is difficult to adjust the τ_f to zero due to the chemical reaction between TiO_2 and $Mg_4Nb_2O_9$ during sintering.

4. Conclusions

The development of crystalline phases and microstructures of $Mg_4Nb_2O_9$-$ZnAl_2O_4$-TiO_2 dielectric ceramics with different phase compositions after sintering has been investigated. The substitution of Al^{3+} and Ti^{4+} for Nb^{5+} in $Mg_4Nb_2O_9$ may promote the decomposition of $Mg_4Nb_2O_9$ into $Mg_5Nb_4O_{15}$. The addition of Ti^{4+} dissolved in $Mg_4Nb_2O_9$ mainly substituted Nb^{5+}, which led to the chemical composition becoming Nb-excess. This in turn resulted in a decrease in the liquidus temperature and promotion

of the densification. The long-range order on the NbO_6 octahedra was enhanced by the co-doping of $ZnAl_2O_4$ and TiO_2 to $Mg_4Nb_2O_9$, thereby increasing the Q×f value. The sample ($0.7Mg_4Nb_2O_9$-$(0.3-x)ZnAl_2O_4$-$xTiO_2$) with x = 0.15-0.2 exhibited a dielectric constant of 13-14, larger than $ZnAl_2O_4$, $Mg_4Nb_2O_9$ and $Mg_5Nb_4O_{15}$. This was due to the larger NbO_6 octahedra distortion resulting from the substitution of Al^{3+}/Ti^{4+} for Nb^{5+} in $Mg_4Nb_2O_9$ and $Mg_5Nb_4O_{15}$. A dielectric constant of 13.1, a high Qxf value of 366,000 GHz and a τ_f of −60.8ppm/°C can be obtained for $0.7Mg_4Nb_2O_9$-0.15 $ZnAl_2O_4$-$0.15TiO_2$ sintered at 1300°C.

Acknowledgment

This work was supported by the Ministry of Science and Technology, Taiwan (MOST 105-2221-E-239-002-). Help with the dielectric properties measurement from Prof. Cheng-Hsing Hsu of the National United University is deeply appreciated. The authors thanks for the English revision of the article from Prof. Arthur Hill of Salford University.

References:

[1] F. Yang, Y. Lai, Y. Zeng, Q. Zhang, J. Han, X. Zhong, H. Su, Ultra-high quality factor and low dielectric constant of $(Zn_{0.5}Ti_{0.5})^{3+}$ co-substituted $MgAl_2O_4$ ceramic, Ceram. Int. 47 (2021) 22522-22529.

[2] A. Ullah, H. Liu, H. Hao, J. Iqbal, Z. Yao, M. Cao, Q. Xu, Effect of Zn substitution on the sintering temperature and microwave dielectric properties of $MgSiO_3$-based ceramics, Ceram. Int. 43 (2017) 484-490.

[3] T. Fujii, A. Ando, Y. Sakabe, Characterization of dielectric properties of oxide materials in frequency range from GHz to THz, J. Eur. Ceram. Soc. 26 (2006) 1857-1860.

[4] M.T. Sebastian, H. Jantunen, Low loss dielectric materials for LTCC applications: a review, Int. Mater. Rev. 53(2008) 57- 90.

[5] R. Peng, H. Su, D. An, Y. Lu, Z. Tao, D. Chen, L.Shi, Y. Li, The sintering and dielectric properties modification of Li_2MgSiO_4 ceramic with Ni^{2+}-ion doping based on calculation and experiment, J. Mater. Res. Tech. 9 (2020) 1344-1356.

[6] R. Peng, Y. Lu, Y. Li, H. Su, L.Shi, G. Yu, Y. Lai, Q. Zao, X. Shi, H. Zhang, Mechanism study of the Mn- substituted magnesium borate: Decreased sintering temperature and improved dielectric property, J. Am. Ceram. Soc. 104(9) (2021) 4614-4623.

[7] H. Ogawa, A. Kan, S. Ishihara and Y. Higashida, Crystal structure of corundum type $Mg_4(Nb_{2-x}Ta_x)O_9$ microwave dielectric ceramics with low dielectric loss, J. Eur. Ceram. Soc. 23 (2003) 2485-2488.

[8] N. Kumada, K. Taki, N. Kinomura, Single crystal structure refinement of a magunesium niobium oxide: $Mg_4Nb_2O_9$, Mater. Res. Bull. 35 (2000) 1017-1021.

[9] A. Yoshida, H. Ogawa, A. Kan, S. Ishihara, Y. Higashida, Influence of Zn and Ni substitutions for Mg on dielectric properties of $(Mg_{4-x}M_x)(Nb_{2-y}Sb_y)O_9$ (M = Zn and Ni) solid solutions, J. Eur. Ceram. Soc. 24 (2004) 1765-1768.

[10] C.L. Huang, J.Y. Chen, C.C. Liang, Dielectric properties of a new ceramic system $(1- x)\ Mg_4Nb_2O_9–xCaTiO_3$ at microwave frequency, Mater. Res. Bull. 44 (2009) 1111-1115.

[11] J.H. Kim, E.S. Kim, Effect of isovalent substitution on microwave dielectric properties of $Mg_4Nb_2O_9$ ceramics, J. Electron. Mater. 48 (2019) 2411–2417.

[12] W. Su, P. Liu, Effects of TiO_2 on microstructure and microwave dielectric properties of $Mg_4Nb_2O_9$ ceramics, Bull. Chin. Ceram. Soc. 25 (2006) 52-57.

[13] K.P. Surendran, N. Santha, P. Mohanan, and M. T. Sebastian, Temperature stable low loss ceramic dielectrics in $(1−x)ZnAl_2O_4–xTiO_2$ system for microwave substrate applications, Eur. Phys. J. B 41 (2004) 301-306.

[14] C.W. Zheng, S.Y. Wu, X.M. Chen, and K.X. Song, Modification of $MgAl_2O_4$ Microwave Dielectric Ceramics by Zn Substitution, J. Am. Ceram. Soc. 90, 1483 (2007).

[15] C.L. Huang, Y.H. Chien, C.Y. Tai, C.Y. Huang, High-Q microwave dielectrics in the $(Mg_{1-x}Zn_x)Al_2O_4$ (x = 0–0.1) system, J. Alloys Compd. 509 (2011) L150–L152.

[16] Y. Li, R. Fu, M. Gao, M. Chen, R. Peng, Y. Lu, Improved $Zn_{0.9}Mg_{0.1}Al_2O_4$ microwave dielectric ceramics with high thermal conductivity, J. Electron. Mater. 50 (2021) 3372-3379.

[17] K.H. Chuang, "Relationships between microstructure and dielectric properties for $Mg_4Nb_2O_9$-$ZnAl_2O_4$-TiO_2 ceramics", undergraduate thesis, National United University, TAIWAN (2017).

[18] R. Peng, Y. Li, Y. Lu, Y. Yun, W. Du, Z. Tao, B. Liao, High-performance microwave dielectric composite ceramics sintered at low temperature without sintering-aids, J. Alloys . Compd. 831 (2020) 154878.

[19] R. Peng, Y. Li, X. Tang, Y. Lu, Q. Zhang, X. Wang, H. Su, Improved sintering and microwave dielectric properties of Li_2CaSiO_4 ceramic with magnesium atom substitution, Ceram. Inter. 46 (2020) 8869-8876.

[20] R. Peng, Y. Li, H. Su, Y. Lu, L.Shi, G. Yu, G. Wang, G. Gan, C. Yu, Three-phase borate solid solution with low sintering temperature, high- quality factor, and low dielectric constant, J. Am. Ceram. Soc. 104 (2021) 3303-3315.

[21] R. Roth, Phase Diagrams for Electronic Ceramics I: Dielectric Ti, Nb, and Ta Oxide Systems, Am. Ceram. Soc. Bull. (1970).

[22] K. Watari, M. C. Valecillos, M.E. Brito, M. Toriyama, S. Kanzaki, Densification and Thermal Conductivity of AIN Doped with Y_2O_3, CaO, and Li_2O, J. Am. Ceram. Soc. 79 (1996) 3103-3108.

[23] C.L. Huang, W.R. Yang, Low-loss microwave dielectrics using $(Mg_{1-x}Zn_x)_4Nb_2O_9$ (x=0.02-0.08) solid solutions, J. Alloys Compd. 509 (2011) 2269-2272.

[24] J. Bezjak, A. Recnik, B. Jancar, P. Boullay, I. R. Evans, D. Suvorov, High-temperature transmission electron microscopy and X-ray powder diffraction studies of polymorphic phase transitions in $Ba_4Nb_2O_9$, J. Am. Ceram. Soc. 92 (2009) 1806-1812.

[25] K. Sarkar, V. Kumar, S. Mukherjee, Synthesis, characterization and property evaluation of single phase $Mg_4Nb_2O_9$ by two stage process, Trans. Indian Ceram. Soc. 76(1) (2017) 43–49.

[26] C.T. Lee, C.C. Ou,Y.C. Lin, C.Y. Huang, and C.Y. Su, Structure and microwave dielectric property relations in $(Ba_{1-x}Sr_x)_5Nb_4O_{15}$ system, J. Eur. Ceram. Soc. 27 (2007) 2273.

[27] C.T. Lee, C.T. Chen, C.Y. Huang, C.J. Wang, Microwave dielectric properties of $(Ba_{1-x}Mg_x)_5Nb_4O_{15}$ ceramics, Jpn. J. Appl. Phy. 47(6R) (2008) 4634-4637.

[28] I.G. Siny, R.W. Tao, R.S. Katiyar, R.A. Guo, and A.S. Bhalla, Raman spectroscopy of Mg-Ta order–disorder in $BaMg_{1/3}Ta_{2/3}O_3$, J. Phys. Chem. Solids 59 (1988)181-195.

[29] I.M. Reaney, Y. Iqbal, H. Zheng, A. Feteira, H. Hughes, D. Iddles, D. Muir, T. Price, Order–disorder behaviour in $0.9Ba([Zn_{0.60}Co_{0.40}]_{1/3}Nb_{2/3})O_3$-$0.1Ba(Ga_{0.5}Ta_{0.5})O_3$ microwave dielectric resonators, J. Eur. Ceram. Soc. 25 (2005) 1183-1189.

[30] H.T. Wu, W.B. Wu, Y.L. Yue, Y.M. Chen, F. Yang, Synthesis and microwave dielectric properties of pseudobrookite-type structure $Mg_5Nb_4O_{15}$ ceramics by aqueous sol–gel technique, Ceram. Int. 38 (2012) 4271–4276

[31] K.P. Surendran, P.V. Bijumon, P. Mohanan, M.T. Sebastian, $(1-x)\ MgAl_2O_4$-$XTiO_2$ dielectrics for microwave and millimeter wave applications, Appl. Phys. A 81 (2005) 823–826.

[32] T.L. Sun, X.M. Chen, Tailoring order-disorder temperature and microwave dielectric properties of $Ba[(Co_{0.6}Zn_{0.4})_{1/3}Nb_{2/3}]O_3$ ceramics, J. Materiomics 2 (2016) 94-100.